



HAKONE XI

11th International Symposium on High Pressure,
Low Temperature Plasma Chemistry



CONTRIBUTED PAPERS

Volume 1

September 7-12, 2008
Oléron Island, France



INVITED PAPERS

IL-1	Non-thermal atmospheric pressure plasmas for aeronautic applications Miles R.B., Opatis D., Shneider M.N., Zaidi S.H.	1
IL-2	Simulation of streamers and sparks in air Naidis G.V.	8
IL-3	Atmospheric Pressure Plasmas for Aerosols Processes in Materials and Environment Borra J.P.	13
IL-4	Recent Advances in the Understanding of Homogeneous Dielectric Barrier Discharges Massines F., Gherardi N., Naudé N., Ségur P.	21
IL-5	Diffuse Coplanar Surface Barrier Discharge and Its Applications for in-line processing of low-added-value materials Černák M., Černáková L., Hudec I., Kováčik D., Zoharanová A.	31

Topic 1: Fundamental Problems of High Pressure Discharges

1-1	Experimental Investigation of Characteristics of an Impulse Streamer Corona Stem Using Artificial Cloud of Charged Aerosol Temnikov A.G., Sokolova M.V., Orlov A.V.	41
1-2	Atmospheric Pressure Generation of $O_2(a^1\Delta_g)$ by Microplasmas Santos Sousa J., Bauville G., Lacour B., Puech V., Touzeau M.	46
1-3	Influence of Surface Charges on Electric Field Distribution in Gas near Dielectric Surface Krivov S.A., Sokolova M.V.	51
1-4	Spatially and Temporally Resolved Emission Spectroscopy of Localized Surface Discharge in Dry Air Sokolova M.V., Kozlov K.V., Krivov S.A., Tatarenko P.A., Samoylovich V.G.	55
1-5	Imaging of streamers propagation on a dielectric surface Allegraud K., Leick N., Guaitella O., Rousseau A.	60
1-6	Radiation Kinetics of the "Hot" Molecules $N_2(C^3\Pi_u)v=0$ in the Barrier Discharge in Humid Argon at Atmospheric Pressure Kozlov K.V., Tatarenko P.A., Samoilovich V.G.	65
1-7	Origin of Vacuum Ultraviolet Light Effective for Synchronization of Positive Surface Streamers Kashiwagi Y., Itoh H.	70
1-8	Efficient models for photoionization produced by streamer discharges in air Célestin S., Liu N.Y., Bourdon A., Pasko V.P., Ségur P., Marode E.	75
1-9	Hexagonal and Honeycomb Structures in Dielectric Barrier Discharges Bernecker B., Callegari T., Blanco S., Fournier R., Boeuf J.P.	80
1-10	Transient spark discharge in air Janda M., Machala Z., Pai D., Stancu G.D., Lacoste D., Laux C.O.	85
1-11	Formation and evolution of the glow-like dielectric barrier discharge at atmospheric pressure Starostin S., ElSabbagh M.A.M., Antony Premkumar P., de Vries H., Paffen R.M.J., Creatore M., van de Sanden M.C.M.	90
1-12	The influence of the flow dynamics on deposition uniformity in Townsend discharge at atmospheric pressure Enache I., Caquineau H., Gherardi N., Naudé N., Massines F.	95

TRANSIENT SPARK DISCHARGE IN AIR

Janda M.^{1a}, Machala Z.^a, Pai D.^b, Stancu G.D.^b, Lacoste D.^b and Laux C.O.^b

a) Division of Environmental Physics, Department of Astronomy, Earth Physics and Meteorology,

Comenius University, Mlynská dolina, Bratislava 842 48, Slovakia

b) Laboratoire E.M2.C CNRS-UPR288, Ecole Centrale Paris, Grande Voie des Vignes, 92295 Châtenay-Malabry, France

Abstract. We have investigated a novel type of streamer-to-spark transition discharge in air at atmospheric pressure named the transient spark (TS), applicable for flue gas cleaning or bio-decontamination. Despite the DC applied voltage, TS has a pulsed character with short (<100 ns) high current (>1 A) pulses, with repetitive frequencies of a few kHz. The emission of N_2 2nd and 1st positive, N_2^+ 1st negative, and atomic N and O lines, was detected. The non-equilibrium character of TS was confirmed by calculated vibrational (3000-5000 K) and rotational (500-1500 K) temperatures. Additionally, temporal emission profiles were obtained using PMT measurements.

1. INTRODUCTION

Atmospheric pressure plasmas in air generated by electrical discharges present considerable interest for a wide range of environmental, bio-medical and industrial applications, such as air pollution control, waste water cleaning, bio-decontamination and sterilization, or material and surface treatment. New types of discharges are therefore still being developed and studied, with a focus on efficiency, power requirements, stability, reliability and simplicity.

Besides measurements of electrical discharge parameters, optical emission spectroscopy (OES) in UV-VIS regions is widely used for plasma diagnostics. It provides valuable information on excited atomic and molecular states, enables to determine the rotational, vibrational, and electronic excitation temperatures of the plasma and thus the level of non-equilibrium and the gas temperature [1,2]. In addition, it enables to identify many radicals and active atomic or molecular species and so gives insight in the plasma chemical processes. This enables understanding and optimizing air or water pollution control processes [3].

2. EXPERIMENTAL SETUP

Experiments were carried out at room temperature in atmospheric pressure air with an axial flow of 10 l/min. The distance between stainless steel needle electrodes in point-to-point configuration varied from 3.5 to 5 mm. A DC High Voltage (HV) power supply HCL 14-20000 connected via a series resistor ($R = 10\text{ M}\Omega$) limiting the total current was used to generate a positive TS discharge. The discharge voltage was measured by a high voltage probe LeCroy PMK-14kVAC and the discharge current was measured using a Pearson Electronics 2877 (1V/A) current probe linked to a 350 MHz digitizing oscilloscope LeCroy Waverunner 434 (maximum 2GS/s).

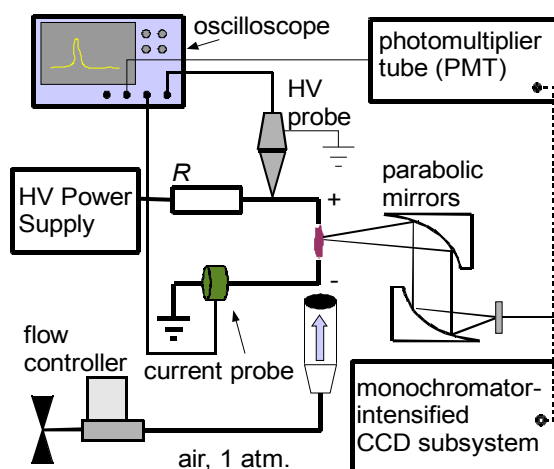


FIGURE 1. Schematic of the experimental set-up, HV - high voltage, R - resistor.

¹ Electronic address: janda@fmph.uniba.sk

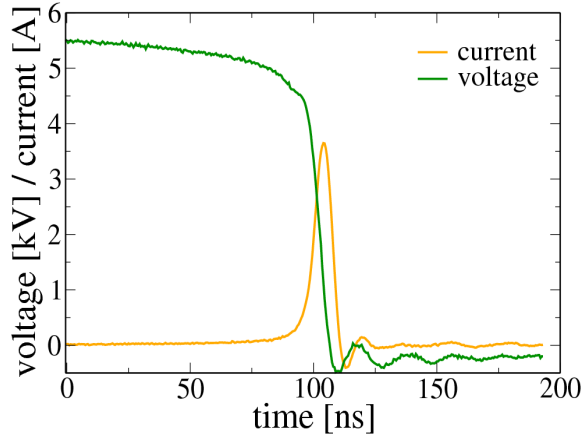


FIGURE 2. Typical TS current and voltage waveforms, repetition frequency ~ 5 kHz.

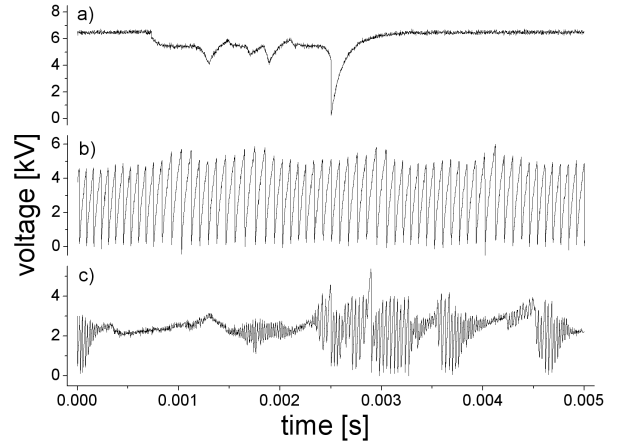


FIGURE 3. Voltage waveforms of different discharge regimes: a) the first random TS pulses , b) regular TS, c) unstable glow regime.

The UV-VIS spectra were obtained using a monochromator (Acton SpectraPro 2500i) fitted with an intensified CCD camera (Princeton Instruments PI-MAX). For time-resolved optical emission measurements, a photomultiplier tube (PMT) module with a 1.4-ns rise time (Hamamatsu H9305-3) was used in place of the monochromator. Its signal was recorded using the oscilloscope. Whenever it was necessary to isolate a specific spectral transition for PMT measurements, a bandpass interference filter (e.g. Melles Griot 03 FIU 127 for the N_2 (C-B 0-0 transition) was inserted into the optical path. The experimental set-up is depicted in Fig. 1.

3. TRANSIENT SPARK

TS is a filamentary streamer-to-spark transition discharge initiated by a streamer, which transforms to a short spark pulse (Fig. 2) due to the discharging of the capacity (C), composed of the internal capacity of the discharge chamber C_{int} , capacity of the HV cable between the resistor R and the HV electrode, and capacity of the HV probe. When C is discharged, the current given by

$$I(t) = -C \times dU/dt \quad (1)$$

reaches a high value (~ 1 A) and the voltage drops to zero due to the resistive fall on the external resistance R . Then, during the quenched phase, C is recharged by a growing potential U on the stressed electrode. The potential U grows in time t according to the following equation:

$$U(t) = U_o [1 - \exp(-t/RC)] \quad (2)$$

where U_o is the high voltage applied to the stressed electrode. Usually, during this relaxation phase when the gap potential crosses a specific threshold, there appears a corona discharge in its glow regime, and some pre-breakdown streamers. As soon as C is sufficiently charged again, it triggers a new pulse. It occurs in time $t = T$, at discharge voltage U_{dis} which is given according to the (2) by:

$$U_{dis} = U_o [1 - \exp(-T/RC)] \quad (3)$$

From the (3) we get the characteristic repetition frequency f of this process:

$$f = 1/T = 1/\{RC \ln[U_o/(U_o - U_{dis})]\}. \quad (4)$$

For typical R and C , the repetition frequency f is in order of several kHz. However, the measured frequency is not absolutely regular. The TS breakdown voltage U_{dis} may also depend on f , especially at higher f , when the electrode's gap may remain pre-ionized. Thus, the next TS breakdown occurs at lower U_{dis} . Lower U_{dis} consequently increases f . As f extends a certain value, TS may transform into a pulse-less glow discharge regime with a constant current of few mA. This transition is controlled by the external resistance R , the distance between the electrodes, and the gas flow rate. Both TS and glow discharge regime are described in more detail in [3,4].

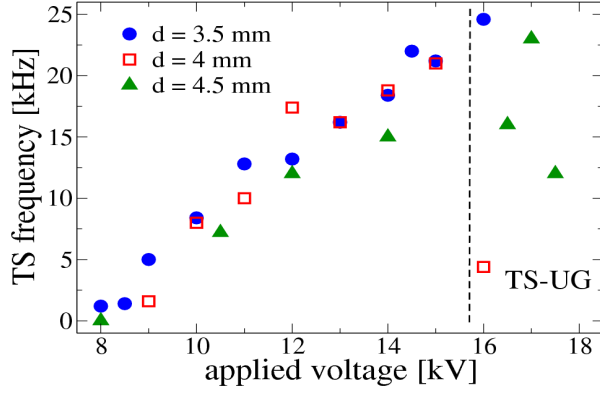


FIGURE 4. Discharge frequency as a function of the applied voltage U_o , TS-UG represents the region of the unstable glow regime, experiments with three different electrode's gaps (d).

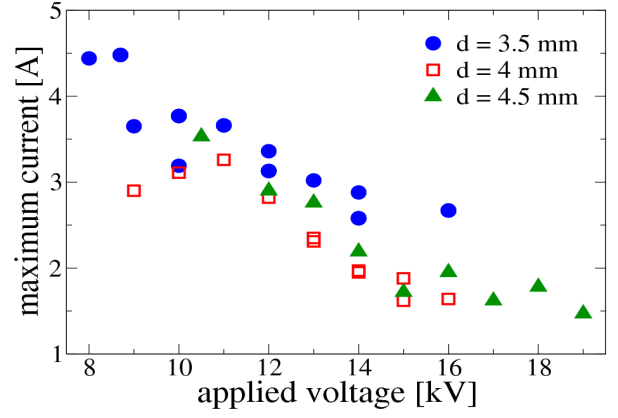


FIGURE 6. Maximum current in pulse I_{max} as a function of applied voltage U_o .

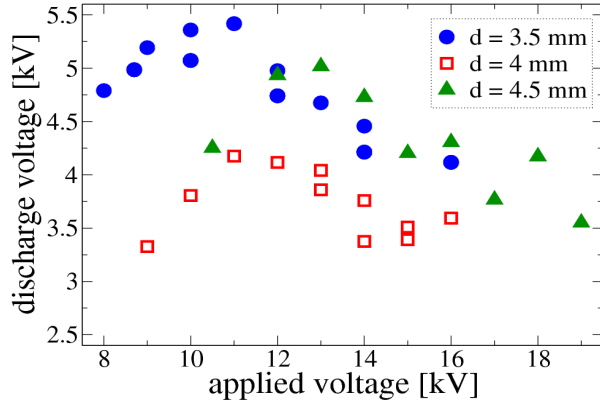


FIGURE 5. Discharge voltage U_{dis} as a function of applied voltage U_o .

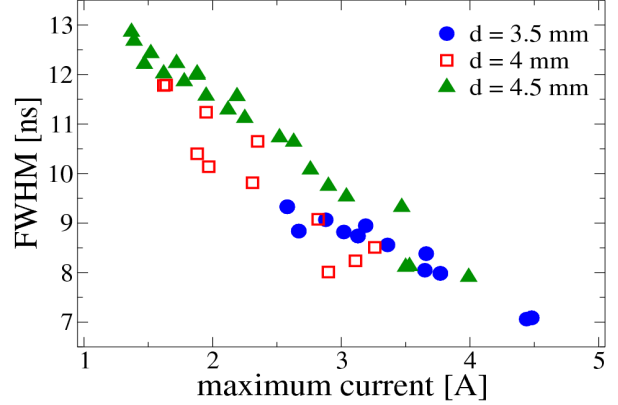


FIGURE 7. Full width of the pulse at half maximum (FWHM) as a function of the maximum current in the pulse (I_{max}).

4. RESULTS AND DISCUSSION

4.1. Electrical characteristics of the discharge

When the high voltage U_o applied to the stressed electrode is progressively increased, we first observe a streamer corona. When the threshold voltage for TS is reached, a transition to TS occurs at the discharge voltage U_{dis} . The repetition frequency (f) of these first TS pulses is low and very irregular (Fig. 3). Further increase of U_o leads to a monotonous increase of f and TS pulses (Fig. 4) become more regular (Fig. 3). However, individual pulses are not identical and U_{dis} , as well as f , vary around their average values.

Figure 5 shows the dependence of the average U_{dis} on U_o . The decrease of U_{dis} for higher U_o can be explained by the increasing gas temperature (Fig. 8), resulting in a decreasing gas density N . Since some threshold reduced electric field E/N is needed to initiate the TS pulse, E and therefore also U_{dis} may be now lowered.

With the increase of U_o , the maximum pulse current (I_{max}) decreases (Fig. 6) and this decrease is accompanied by the broadening of the pulses (Fig. 7). As a result, no significant dependence of the integrated current per pulse (Q) on U_o is observed, and due to the increasing f the mean discharge current (I_{mean}) increases linearly with U_o . When the frequency exceeds around 20 kHz, the discharge tends to convert to the glow regime. However, due to the high value of R and the electro-negativity of air, this regime is not stable and the discharge randomly switches between the glow regime and the high frequency TS regime (Fig. 3).

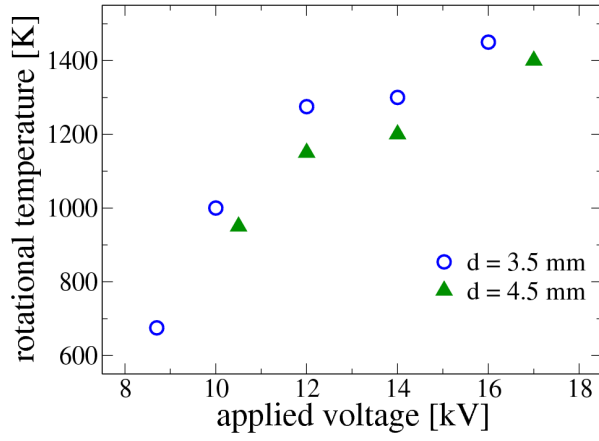


FIGURE 8. Rotational temperature measured from N_2 (C-B, 0-0) as a function of U_o .

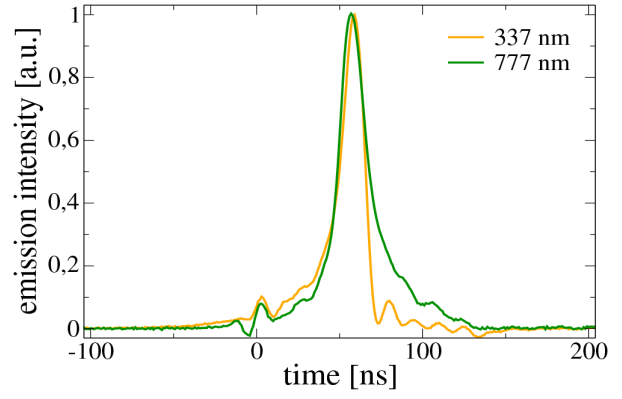


FIGURE 100. Normalized temporal emission profiles obtained by PMT with filter for N_2 (C-B, 0-0) (337 nm) and O^* (777 nm), time $t = 0$ ns represents the maximum of the current pulse.

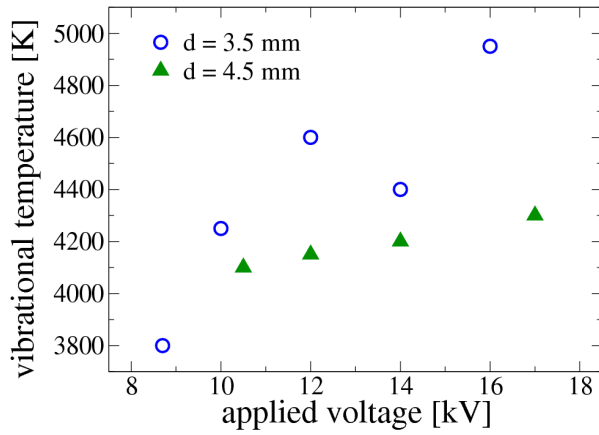


FIGURE 9. Vibrational temperature of $N_2(C)$ species as a function of U_o .

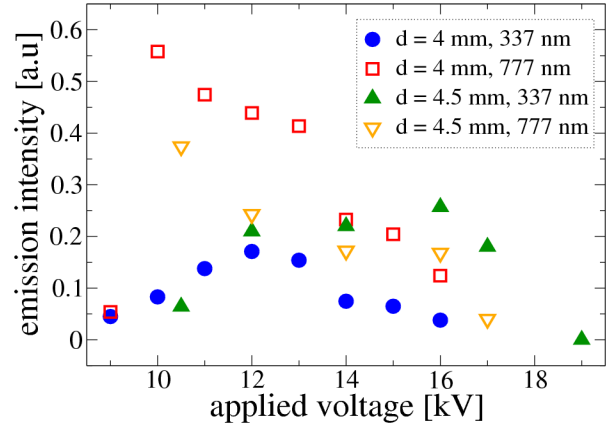


FIGURE 111. Maximum of emission of N_2 (C-B, 0-0) (337 nm) and O^* (777 nm) obtained by PMT as a function of U_o .

TS is based on the charging and discharging of C , the integrated current Q and the energy delivered to the discharge gap per pulse (E_p) are therefore functions of U_{dis} and they can be expressed as

$$Q = CU_{dis} \quad (5)$$

and

$$E_p = CU_{dis}^2/2 \quad (6)$$

respectively. The knowledge of the value of C is therefore important for the description and characterization of TS. First, we calculated C by fitting the obtained current waveforms with current obtained as a negative derivate of the measured voltage waveforms (Eq. 1). By this way we found C to be 6.3 ± 0.3 pF. The values of Q and E_p calculated from equations (5) and (6), respectively, using this value of C are in agreement with Q and E_p obtained by the integration of $I(t)$ and $U(t)I(t)$ for the whole period of the current pulse. On the other hand, this value of C significantly overestimates the TS repetition frequency calculated from equation (4).

We therefore calculated C also from the growth of the voltage on the stressed electrode during the relaxation period (Eq. 2). We obtained another value of $C = 14 \pm 1$ pF, which enables a correct calculation of f . As a result, we have two values of C , the lower one suitable for the description of discharging event and the second one suitable for the description of charging period. The understanding of this phenomenon requires further study.

4.2. Emission study

In the UV-VIS emission spectra of TS, the strongest lines observed can be attributed to the emission of N_2 2nd positive system ($C^3\Pi_u - B^3\Pi_g$) and atomic O line (at 777 nm). Emission of N_2 1st positive system ($B^3\Pi_g - A^3\Sigma^+$), N_2^+ 1st negative system ($B^2\Sigma^+ - X^2\Sigma^+$), and atomic N lines is also observed. The presence of N_2^+ and atomic lines indicate that the plasma has high electron temperature and a significant level of non-equilibrium. Non-equilibrium conditions are also confirmed by a difference between the vibrational (T_v) and rotational (T_r) temperatures obtained by fitting the experimental spectra of N_2 2nd positive system with the simulated ones (using the Specair program [6]).

The degree of non-equilibrium probably decreases with increasing U_o , because T_r increases from about 500 K to 1500 K (Fig. 8) and T_v increases from about 3800 K to 5000 K (Fig. 9). On the other hand, the mean electron temperature (T_e) most probably decreases with increasing U_o , since the intensity of atomic O emission per pulse decreases with U_o (Fig. 11). The unstable glow regime probably leads to an even more significant decrease of T_e , because in this regime even the emission of N_2 2nd positive system decreases markedly.

The temporal emission profiles obtained using the PMT measurements also reveal that the maximum intensity of emission lags approximately 60 ns behind the current pulse maximum and the emission of N_2 2nd positive system is quenched faster than the emission of atomic O (Fig. 10).

5. CONCLUSIONS

We investigated electrical characteristics and emission spectra of a DC-supplied periodic streamer-to-spark transition discharge in atmospheric air, called transient spark (TS). Thanks to the very short spark pulse duration given by the small internal capacity of the discharge chamber and a limiting series resistor, the plasma generated by TS cannot reach LTE conditions. The periodic streamer-to-spark transition provides non-equilibrium conditions with fast electrons resulting in strong chemical effects. The existence of non-equilibrium conditions is also confirmed by the inferred vibrational and rotational temperatures.

TS in air generates N_2 excited species, N and O atoms, and N_2^+ ions. The low frequency mode with stronger and shorter current pulses apparently generates higher concentrations of radicals per pulse. However, due to increasing average repetition frequency, the regime with pulses of average amplitude and repetition frequency around 10 kHz, where the strongest emission of N_2 2nd positive system was observed, seems the most suitable for the chemical effects.

ACKNOWLEDGMENTS

Research was supported by Slovak grant agency VEGA 1/0293/08, NATO EAP.RIG 981194, and EOARD FA8655-08-1-3061 grants.

REFERENCES

Journals

- [1] C.O. Laux, T.G. Spence, C.H. Kruger, R.N. Zare, *Plasma Sources Sci. Technol.*, **12**, 125 (2003)
- [2] U. Fantz, *Plasma Sources Sci. Technol.*, **15**, S137 (2006)
- [3] Z. Machala, M. Janda, K. Hensel, I. Jedlovsky, L. Lestinska, V. Foltin, V. Martisovits, M. Morvová, *J. Mol. Spectrosc.*, **243**, 194 (2007)
- [4] Z. Machala, I. Jedlovsky and V. Martisovits, *IEEE Trans. Plasma Sci.*, **36**, in press (2008)
- [5] Z. Machala, E. Marode, C.O. Laux, C.H. Kruger, *J. Adv. Oxid. Technol.*, **7**, 133 (2004)

Reports and Theses

- [6] C.O. Laux, *Radiation and Nonequilibrium Collisional-Radiative Models*, von Karman Institute for Fluid Dynamics, Lecture Series 2002-07, Rhode Saint-Genese, Belgium, 2002



Université Paul Sabatier

118, route de Narbonne 31062 TOULOUSE Cédex 09
Tél : 05.61.55.66.12 – Fax : 05.61.55.64.31